Title: In Vitro Structure-Activity Relationship Determination of 30 Psychedelic New Psychoactive Substances by Means of Beta-Arrestin 2 Recruitment to the Serotonin 2A Receptor

Authors: Pottie, Eline, Annelies Cannaert, and Christophe Stove

In: ARCHIVES OF TOXICOLOGY 94 (10): 3449–3460, 2020

In vitro structure-activity relationship determination of 30 psychedelic new psychoactive substances by means of β-arrestin 2 recruitment to the serotonin 2A receptor

Eline Pottie, Annelies Cannaert and Christophe P Stove*

Laboratory of Toxicology, Department of Bioanalysis, Faculty of Pharmaceutical Sciences, Ghent University, Campus Heymans, Ottergemsesteenweg 460, B-9000 Ghent, Belgium.

* Corresponding Author: Christophe Stove, Laboratory of Toxicology, Department of Bioanalysis, Faculty of Pharmaceutical Sciences, Ghent University, Ottergemsesteenweg 460, 9000 Ghent, Belgium, Phone: +32 9 264 81 35, Fax: +32 9 264 81 83, E-mail: christophe.stove@UGent.be

Abstract:

Serotonergic psychedelics, substances exerting their effects primarily through the serotonin 2A receptor (5-HT_{2A}R), continue to comprise a substantial portion of reported new psychoactive substances (NPS). The exact mechanisms of action of psychedelics still remain to be elucidated further, and certain pathways remain largely unexplored on a molecular level for this group of compounds. A systematic comparison of substances belonging to different subclasses, monitoring the receptor-proximal β-arrestin 2 recruitment, is lacking. Based on a previously reported *in vitro* bioassay employing functional complementation of a split nanoluciferase to monitor β-arrestin 2 recruitment to the 5-HT_{2A}R, we here report on the set-up of a stable HEK 293T cell-based bioassay. Following verification of the performance of this new stable cell system as compared to a system based on transient transfection, the stable expression system was deemed suitable for the pharmacological characterization of psychedelic NPS. Subsequently, it was applied for the *in vitro* assessment of the structure-activity relationship of a set of 30 substances, representing different subclasses of phenylalkylamine psychedelics, among which 12 phenethylamine derivatives (2C-X), 7 phenylisopropylamines (DOx) and 11 N-benzylderivatives (25X-NB). The resulting potency and efficacy values provide insights into the structure-activity relationship of the tested compounds, overall confirm findings observed with other reported *in vitro* assays, and even show a significant correlation with estimated common doses. This approach, in which a large series of psychedelic NPS belonging to different subclasses is comparatively tested, using a same assay set-up, monitoring a receptor-proximal event, not only gives pharmacological insights, but may also allow prioritization of legal actions related to the most potent -and potentially dangerous- compounds.

Keywords: bioassay, structure-activity relationship, serotonin receptor, hallucinogen, new psychoactive substances, psychedelic

Introduction

In early 2020, a cumulative total of 950 new psychoactive substances (NPS) had been reported to the United Nations Office on Drugs and Crime (UNODC). Over the years, the group of serotonergic psychedelics has consistently comprised a substantial portion of these newly reported substances (UNODC 2020). The term serotonergic psychedelics includes compounds that exert their pharmacological effects mainly via the serotonin $(5\text{-HT})_{2A}$ receptor (5-HT_{2A}R)(Nichols 2004; Nichols 2016). This structurally diverse class can be divided into three subclasses: the tryptamines (for example the naturally occurring psilocybin), the ergolines (such as the semisynthetic lysergic acid diethylamide (LSD)), and the phenylalkylamines (with mescaline as the prototypical substance)(Nichols 2018). Within the latter group, prominent substances can be found in subgroups, such as the 2C psychedelics (e.g. 2C-B), the phenylisopropylamines (psychedelic amphetamines, shortly DOx, e.g. DOB), and the N-benzyl derivatives of those groups (e.g. 25B-NBOMe and 25B-NBOH)(Poulie et al. 2019).

The effects sought for by users, common to all serotonergic psychedelics, include mystical experiences, alterations in consciousness, empathic feelings, and sensory and somatic effects. However, severe adverse effects can occur, among which agitation, tachycardia, hyperthermia, rhabdomyolysis, hypertension and seizures (Dean et al. 2013; Hondebrink et al. 2018; Kyriakou et al. 2015; Suzuki et al. 2015). With the more recent group of NBOMes, a number of case reports requiring hospitalization, suicide attempts and even deaths have been reported (Hondebrink et al. 2018; Kyriakou et al. 2015; Luethi and Liechti 2020; Suzuki et al. 2015). Furthermore, a mass poisoning has been reported with Bromo-DragonFLY and 2C-E (Iwersen-Bergmann et al. 2019). The potential risks associated with phenethylamine psychedelics have been emphasized by Risk Assessment Reports of the European Monitoring Centre for Drugs and Drug Addiction (EMCDDA) for 2C-I, 2C-T-2, 2C-T-7 and 25I-NBOMe (EMCDDA-Europol 2014; EMCDDA 2004).

The main pharmacological target of serotonergic psychedelics, the 5-HT_{2A}R, is a G protein-coupled receptor (GPCR)(Canal 2018; Nichols 2004). Activation of the 5-HT_{2A}R induces an interaction of the receptor with the G protein, in this particular case $G\alpha_q$. This results in a series of downstream signaling events, among which the activation of phospholipase C (PLC), with an associated increase in inositol phosphate (IP) levels, and mobilization of intracellular Ca^{2+}. Furthermore, the receptor can induce arachidonic acid release through phospholipase A (PLA) activation. Besides the activation of the canonical G protein pathway, also β-arrestin 2 (βarr2) is recruited to the activated GPCR. This scaffolding protein can induce the desensitization and/or internalization of the receptor, and is

responsible for a distinct set of signaling events (Canal 2018; Lopez-Gimenez and Gonzalez-Maeso 2018; Nichols 2016).

To date, it remains elusive which (combination) of these events is responsible for the typical effects exerted by serotonergic psychedelics. A more thorough pharmacological characterization of these substances is undeniably required, as e.g. apart from LSD, the βarr2 recruitment of psychedelic substances by the 5-HT_{2A}R has only been scarcely explored on a molecular level (Pottie et al. 2019; Wacker et al. 2017). In earlier structure-activity relationship assessments, the focus mostly lay on binding studies, supplemented with functional assays employing Ca^{2+} mobilization, PLC and PLA activity as the readout method (Braden et al. 2006; Canal 2018; Elmore et al. 2018; Hansen et al. 2014; Kolaczynska et al. 2019; Luethi et al. 2018; Luethi et al. 2019; Moya et al. 2007; Parrish et al. 2005; Rickli et al. 2015; Rickli et al. 2016). The use of different methods severely complicates the interpretation and comparison of results obtained in different studies, which may also explain apparent discrepancies in reported conclusions. One of the underlying reasons may be differences in 'receptor reserve' between distinct functional assays, in which saturation of a readout may already be achieved with lower ligand concentrations or following stimulation with a partial agonist in one assay, but not in the other. As such saturation may typically be observed when using assays that score events further downstream, receptor-proximal assays are preferred to evaluate a compound's intrinsic receptor activating potential (Kurrasch-Orbaugh et al. 2003; Wouters et al. 2019). Thus, ideally, to comprehensively compare different substances, the same experimental setup is used, preferentially a bioassay that scores a receptor-proximal event. Therefore, in this study, a stable cell system was developed that allows to monitor the interaction of βarr2 with the activated 5-HT_{2A}R, an upstream signaling event, using a luminescent readout (Nanoluciferase Binary Technology, NanoBiT®). The newly developed system was first compared with its previously reported counterpart based on transient transfection of cells (Pottie et al. 2019). Subsequently, it was used for the comparative pharmacological characterization of an extensive set of psychedelic phenylalkylamines, comprehensively including substances from three subclasses of this group: 12 2C-X, 7 DOx and 11 NBOMe/NBOH compounds. Also, the correlation of the obtained EC_{50} values with recreational dose estimates was assessed.

Materials and methods

- **Chemicals and reagents**

Hank's Balanced Salt Solution (HBSS), Phosphate Buffered Saline (PBS), Dulbecco's Modified Eagle's Medium (DMEM) supplemented with GlutaMAX®, penicillin/streptomycin (5 000 U/mL), amphotericin B (250 µg/mL), trypsin, DOTAP transfection reagent, Phusion High-Fidelity PCR Master Mix, T4 DNA ligase and the restriction enzymes *BamH*I and *SnaB*I were procured from Thermo Fisher Scientific

(Pittsburg, PA, USA). Transfection reagent FuGENE® was from Promega (Madison, WI, USA). The anti-dNGFR (truncated nerve growth factor receptor) antibody was purchased from Chromaprobe (Maryland Heights, MO, USA). Cloning primers, poly-D-lysine hydrobromide, Fetal Bovine Serum (FBS), and the analytical standards of LSD (lysergic acid diethylamide) and serotonin were purchased from Sigma Aldrich (Overijse, Belgium). The remaining analytical standards, with the chemical names and original manufacturers provided in Table S1 in Supplementary Data, and the structures shown in Figure 1 and Table 2, were provided by Chiron AS (Trondheim, Norway), Cayman Chemical Company (Ann Arbor, MI, USA), LGC standards (Teddington, UK), and the Australian Government National Measurement Institute (West Lindfield, Australia). The analytical standards of 2C-B, 2C-C, 2C-I, 25B-NBOMe, 25C-NBOMe and 25I-NBOMe were a kind gift of prof. K. Maudens (University of Antwerp). The analytical standard of Bromo-dragonFLY was kindly provided by Chiron AS. For chiral compounds (DOx), the racemic mixture was purchased.

- **Cell culture**

Human Embryonic Kidney (HEK) 293T cells were routinely cultured in DMEM (GlutaMAX®), supplemented with 10 % heat-inactivated FBS, 100 IU/mL of penicillin, 100 µg/mL streptomycin and 0.25 µg/mL amphotericin B. The cells were maintained in a humidified atmosphere, at 37°C and 5 % CO_2.

- **Cloning of the 5-HT_{2A}R-LgBiT construct into pLZRS-IRES-EGFP**

The development and selection of the optimal combination of 5-HT_{2A}R and βarr2 constructs in the NanoBiT® system was described previously (Pottie et al. 2019). In order to reduce the time and variability associated with transient transfection, a stable cell system, stably expressing the 5-HT_{2A}R-LgBiT and SmBiT-βarr2 constructs, was generated via viral transduction. To this end, the 5-HT_{2A}R-LgBiT construct was subcloned into the pLZRS-IRES-EGFP vector. This vector was digested with the restriction enzymes *BamH*I and *SnaB*I, and purified via gel electrophoresis and subsequent extraction using an E.Z.N.A.® MicroElute Gel Extraction Kit (VWR International, Radnor, PA, USA). Hundred pg of template plasmid DNA containing the 5-HT_{2A}R-LgBiT construct was mixed with the forward and reverse primers (ACTCAA*GGATCC*ACCATGTACCCATACGATGTTCC and ACTCAA*TACGTA*TTAGCTGTTGATGGTTACTCGG, respectively; restriction sites underlined) at a final concentration of 0.5 µM with PCR Mastermix. The 3-step PCR reaction was carried out in a Mastercycler™ Nexus Thermal Cycler (Eppendorf, Hamburg, Germany), using the following conditions: initial denaturation (30 s at 98°C), denaturation (10 s at 98°C), annealing (20 s at 70.1°C), extension (1 min at 72°C) and final extension (5 min at 72°C), for which the three middle steps were repeated 32 times. The PCR product was subjected to gel electrophoresis and subsequent purification, followed by restriction digestion with enzymes *BamH*I

and *SnaB*I, and purification with an E.Z.N.A.® MicroElute Cycle Pure Kit (VWR International). After dephosphorylation of the digested vector by Thermosensitive Alkaline Phosphatase (Promega), the vector and insert were ligated using T4 DNA Ligase. After transformation, chemically competent *E. coli* bacteria were plated on ampicillin-containing agar plates and left to grow overnight. The resistant colonies were screened via PCR, grown in Luria Bertani broth with ampicillin (100 µg/mL) and the plasmids were purified using E.Z.N.A.® Plasmid DNA Mini Kit (VWR International). The correctness of the construct was verified via restriction digest and Sanger sequencing.

- **Generation of a stable cell line, using the viral construct**

The generation of the 5-HT_{2A}R-LgBiT virus was performed in a Phoenix packaging cell line using the same protocol as used for the generation of the previously developed virus containing the SmBiT-βarr2 construct (Cannaert et al. 2017). Equal quantities of the two viral supernatants were used to transduce HEK 293T cells, using DOTAP liposomal transfection reagent. To increase the transduction efficiency, the cells were subsequently centrifuged for 90 min (950 g, 32°C). A flow cytometric analysis was performed to estimate transduction efficiency in the cells, via the markers EGFP (Enhanced Green Fluorescent Protein, co-expressed with 5-HT_{2A}R-LgBiT) and dNGFR (truncated Nerve Growth Factor Receptor, co-expressed with SmBiT-βarr2). For the latter, a fluorescently labelled anti-dNGFR antibody was used. The cells expressing the highest levels of the two constructs were selected via flow-cytometry assisted cell sorting (FACS) of these co-expression markers, using a BD FACSAria III cell sorter (BD Biosciences, Erembodegem, Belgium), equipped with 405, 488, 561, and 640 nm lasers. During the course of experiments, the expression levels of the introduced constructs were monitored through flow cytometry, and found to be stable until (at least) passage 10.

- **βarr2 recruitment assay in transiently transfected HEK 293T cells**

The bioassay monitoring the recruitment of βarr2 to the 5-HT_{2A}R using transient transfection, was carried out as described before (Cannaert et al. 2016; Pottie et al. 2019). Briefly, routinely cultured HEK 293T cells were seeded in 6-well plates, at a density of 500 000 cells per well. The day after, 1.65 µg of both the SmBiT-βarr2 and the 5-HT_{2A}R-LgBiT construct were transiently transfected using a 3:1 FuGENE®:DNA ratio, according to the manufacturer's protocol. Twenty-four hours post-transfection, the cells were reseeded into poly-D-lysine coated 96-well plates, at a density of 50 000 cells per well. The next day, the cells were washed twice with HBSS, and 100 µL HBSS was pipetted into each well. To this, 25 µL of NanoGlo Live Cell Reagent (diluted 1/20 in the provided buffer, according to the manufacturer's protocol) was added, followed by an equilibration stage in the Tristar^2 LB 942 multimode microplate reader (Berthold Technologies GmbH & Co, Germany). Upon stabilization of the

signal, 10 µL of 13.5 x concentrated agonist solution was added, and luminescent signals were monitored for 2 hours.

- **Stable βarr2 recruitment bioassay for the pharmacological characterization of psychedelics**

The bioassay protocol using the generated cell line stably expressing 5-HT_{2A}R-LgBiT and SmBiT-βarr2, is similar to the latter two days of the protocol with transient transfection (Cannaert et al. 2017). In brief, the cells are seeded in 96-well plates at a density of 50 000 cells per well and incubated overnight. The cells are rinsed twice with HBSS, 100 µL of HBSS and 25 µL of diluted NanoGlo Live Cell Reagent are pipetted into each well. After the equilibration phase, 10 µL of 13.5 x concentrated agonist solution was added, obtaining final in-well concentrations of (100 µM) – (25 µM) – (10 µM) – 1 µM – 100 nM – 10 nM – 1 nM – 100 pM – 10 pM – (1 pM). Luminescence was monitored for 2 hours. Solvent controls were run for all tested conditions, and each compound was tested at least in three independent experiments, each performed in duplicate.

- **Data processing and statistical analysis**

Concentration-response curves were generated by correcting the obtained time profiles for inter-well variability, calculating the area under the curve (AUC), and subtracting the AUC of the corresponding solvent control, as described before in more detail (Pottie et al. 2020). For normalization of the data to the reference compound LSD (E_{max} = 100%) and curve fitting of the sigmoidal concentration-response curves, the four parametric non-linear regression model was used in GraphPad Prism software (San Diego, CA, USA). Statistical significance of differences between obtained results was determined via Mann-Whitney U analysis in GraphPad Prism.

A correlation factor was determined between an estimated common dose for recreational use, and the obtained EC_{50} value of the substance in the described bioassay. The dose estimate was calculated as follows: for all tested compounds, the mean of the common doses was searched in PiHKAL, and on specific websites (erowid.org, tripsit.me and psychonautwiki.org), similarly as described in Luethi and Liechti (Luethi and Liechti 2018; Shulgin and Shulgin 1991). From these ‘mean common doses’, the median value was calculated, and used in the correlation test as ‘dose estimate’. Substances for which no relevant doses were found in the aforementioned sources, were not included in the analysis. A correlation coefficient was determined via the Pearson rank order correlation coefficient, via GraphPad Prism.

Results

- **Generation and validation of a new stable cell system**

To determine the structure-activity relationship of phenylalkylamine psychedelics in terms of βarr2 recruitment to the 5-HT_{2A}R, the NanoBiT® (Nanoluciferase Binary Technology) system was employed, a technique designed to monitor protein-protein interactions in live cells in real-time. This technology employs a nanoluciferase enzyme that is split in two parts, each of these being fused to proteins that may potentially interact, in this case the 5-HT_{2A}R and βarr2. In the presence of an agonist, βarr2 is recruited to the activated receptor, thereby inducing functional complementation of the enzyme, generating a luminescent signal in the presence of its substrate (Dixon et al. 2016). The selection of the optimal combination of receptor and βarr2 constructs (5-HT_{2A}R-LgBiT with SmBiT-βarr2) was described previously (Pottie et al. 2019). In order to reduce the hands-on time and the variability associated with transient transfection, a stable cell system, stably expressing the 5-HT_{2A}R-LgBiT and SmBiT-βarr2 constructs, was generated.

To validate the performance of the newly developed cell line, we first tested the concentration-dependence of the endogenous agonist serotonin and the prototypical psychedelic substance LSD in the bioassay. As depicted in Figure 2A, both agonists induce responses that enable the generation of a sigmoidal concentration-response curve, and the calculation of an EC_{50} and E_{max} value. Contrarily to reports in literature, the E_{max} values of LSD and serotonin are comparable, yielding an EC_{50} of 37.2 nM and an E_{max} of 113 % for serotonin (the latter value normalized to the E_{max} of LSD)(Nichols 2004). An explanation can be found in the different course of the profiles generated by the highest concentration (10 µM) of the respective agonists, as shown in Figure 2B. Several typically used bioassays employ an endpoint measurement as a readout. Also in our bioassay, serotonin reaches higher absolute signals than LSD, as would be monitored with an endpoint measurement assay, only taking into account the signal at a given time point. However, the full activation profile yields an AUC for serotonin that is only slightly higher than that of LSD. For consistency with our previous reports, the full 2h readout was employed for the calculation of the AUC, and LSD was selected as the reference agonist, given the higher relevance of this prototypical psychedelic compound in the context of psychedelic NPS.

Subsequently, a small set of compounds was tested simultaneously in both the transiently transfected and stably transduced cell systems, to assess the comparability of the obtained results. The structures are shown in Figure 1, where the R-substitutions refer to those given in Table 2. Figure 2 depicts the obtained concentration-response curves, and Table 1 provides the associated EC_{50} and E_{max} values, as a measure of potency and efficacy of a compound, respectively. As can be seen in Figure 2, the curves obtained with the stable cell system (right panel) allow for the same conclusions as those obtained using the transiently transfected cells (left panel). The data in Table 1 further support this finding, and

are highly comparable with our previously published data (Pottie et al. 2019), adding to the robustness of the bioassay.

- **Pharmacological characterization and structure activity-relationship determination of structurally distinct sets of phenylalkylamine psychedelics**

Following the favorable evaluation of the newly developed stable cell system, this 5-HT_{2A}R bioassay was employed for the pharmacological characterization (determination of EC_{50} and E_{max} values) of sets of 2C-X, DOx and N-benzyl-derived compounds (25X-NB). Table 2 provides an overview of the structural properties of the tested compounds, where the places of substitution (R^{1-7}) refer to Figure 1. This Table also lists all the evaluated compounds' EC_{50} (as a measure of potency) and E_{max} (as a measure of efficacy) values, the latter calculated with the full 2h activation profiles. Table S2 in Supplementary Data includes the E_{max} values calculated using only the first 30 min of this full activation profile for LSD, serotonin and a subset of compounds from the different subclasses, yielding efficacies with overlapping confidence intervals. This consistency adds to the robustness of the bioassay.

Discussion

Although many serotonergic psychedelics have appeared on the drug market over the past few years, these compounds and their mechanism(s) of action remain incompletely described. The definition of the structure-activity relationship of these substances at their main target receptor, 5-HT_{2A}R, has been mostly based on their binding affinities and using assays focusing on functional outcomes such as Ca^{2+} mobilization and PLA and PLC activation, events lying further downstream the signaling cascade. Meanwhile, a comprehensive comparison of different subgroups of phenylalkylamine psychedelics in one single assay format, monitoring a receptor-proximal signaling event like the recruitment of βarr2 to the 5-HT_{2A}R, is lacking (Braden et al. 2006; Canal 2018; Elmore et al. 2018; Eshleman et al. 2018; Hansen et al. 2014; Moya et al. 2007; Parrish et al. 2005; Rickli et al. 2015). Therefore, we developed a stable cell system that allows for the monitoring of this recruitment, through the functional complementation of a split nanoluciferase enzyme. We first ascertained that the data generated with the newly developed stable cell line were similar to those obtained via a simultaneously executed assay using transiently transfected cells, as previously described (Pottie et al. 2019). The results are shown in Figure 2 and Table 1. As the data obtained with both assays were similar and in line with our previously published data, the newly developed cell system was deemed suitable for the pharmacological characterization and comprehensive structure-activity relationship determination of an extensive set of compounds encompassing three subgroups of phenylalkylamine psychedelic

substances. Additionally, we assessed the correlation between the obtained EC_{50} values of these psychedelics, and their estimated common doses.

1. Phenethylamine psychedelics (2C-X)

Phenethylamines are characterized by a phenyl group linked to an amine function by a 2-carbon (ethyl) alkyl chain. Although technically not a 2C-X compound, the best described phenethylamine psychedelic is the naturally occurring mescaline, bearing three methoxy groups on the phenyl moiety, at positions 2,3 and 4 ($R^{1\text{-}2}$ in Figure 1 and Table 2, which define the structures of the tested substances). This substitution pattern resulted in a low potency (2659 nM) and efficacy (maximal response of 55.5 %), matching with our previous findings (Pottie et al. 2019), and with literature (Blaazer et al. 2008; Braden et al. 2006; Nichols 2004; Rickli et al. 2015). Therefore, the substitution pattern found in the naturally occurring mescaline was mostly replaced by a 2,5-dimethoxy pattern in the newer synthetic analogues (2C-X, and also in the DOx compounds), in an effort to create more potent substances (Blaazer et al. 2008; Nichols 2018; Shulgin and Shulgin 1991). All concentration response-curves of the 2C-X compounds (and mescaline) can be found in Supplementary Figure S1.

The most simple 2C derivative, 2C-H (Figure 1 and Table 2), with a 2,5-dimethoxy pattern on the phenyl moiety, is only marginally active at the $5\text{-}HT_{2A}R$, with an EC_{50} value above 2 µM, and a maximal efficacy of 67.4 % (compared to the E_{max} of the reference agonist LSD, defined as 100 %). As described further, a series of structural modifications of this compound clearly influence the activity: substitutions at (i) position 4 of the phenyl group (R^1), (ii) the β-position of the phenethylamine (R^4) and the amine group (R^6), and (iii) the tethering of the methoxy groups in a tetrahydrofuran heterocyclic ring structure.

An impactful substitution lies in the addition of a 4-substituent (R^1) on the phenyl group (the –X in 2C-X, DOx and 25X-NB, as depicted in Figure 1 and Table 2). These are mostly lipophilic groups. In this study the halogens Br, I and Cl, methyl (D) and ethyl (E) groups, and alkylthio groups (T-2 and T-7) were included. Our bioassay indicated a marked increase in potency and efficacy for all compounds, when compared to the unsubstituted counterpart (2C-H). The positive effect of 4-substituents (R^1) on the potency and binding affinity of 2C psychedelics in *in vitro* assays was also already reported in literature (Blaazer et al. 2008; Braden et al. 2006; Rickli et al. 2015). The substitution with alkylthio groups at this position (2C-T-2 and 2C-T-7) yielded the highest efficacies within the 2C-X group, a consistent finding in the βarr2 bioassay and previous literature (Nichols 2018). For 2C compounds with halogenated R^1 (2C-C, 2C-B and 2C-I) and alkyl R^1 substituents (2C-D and 2C-E), the potencies were in the low nanomolar range and the efficacy ranged over a rather small interval between 70.6 and 91.2 %. The potency increased (from an EC_{50} value of 43.5 to 6.88 nM) when the methyl group of 2C-D was replaced

by a longer ethyl function (2C-E), an effect observed by others as well (Blaazer et al. 2008; Rickli et al. 2015).

Concerning the β position and amine function (R^4 and R^6 in Figure 1 and Table 2), certain substitutions of the phenethylamine structure can have a negative impact on the potency and/or efficacy. The introduction of a keto group at the β position of the phenethylamine (R^4) was previously reported to strongly reduce the *in vivo* activity (Blaazer et al. 2008). Here, we demonstrated that the introduction of a keto group at the β position (R^4) yields a compound that is *intrinsically* less active at the 5-HT_{2A}R, as evidenced by the strongly reduced potency and efficacy of β-k-2C-B (905 nM and 40.8 % respectively), when compared to 2C-B (9.03 nM and 89 %). A second example lies in the addition of a small methyl group at the amine position (R^6) of the phenethylamine (Blaazer et al. 2008; Braden et al. 2006). As can be seen for N-Me-2C-H, this resulted in a slight reduction of both potency (4464 nM) and efficacy (41.2%) compared to the 2C-H counterpart (2408 nM; 67.4 %).

The tethering of the two methoxy groups of 2C-B into two structurally rigidified tetrahydrofuran heterocyclic rings yields 2C-B-FLY, of which the structure is shown separately in Figure 1, and the obtained potency and efficacy data are included in Table 2. This ring structure did not markedly influence the activity of the compound in terms of βarr2 recruitment, yielding similar EC_{50} (9.03 nM for 2C-B and 8.11 nM for 2C-B-FLY) and E_{max} values (89 % and 81.8 %, respectively), for the two compounds. The equipotency upon tethering of the two methoxy groups into a tetrahydrobenzodifuran moiety corresponds with previous findings in literature (Halberstadt et al. 2019).

2. Phenylisopropylamine psychedelics (psychedelic amphetamines, DOx)

The addition of a methyl group at the α-position (R^5) of the phenethylamine (2C-X) leads to the formation of phenylisopropylamine (DOx) compounds, which have similar potencies and markedly increased efficacies compared to the 2C-X derivatives. The trend is consistently seen among the compounds with different R^1-substituents (2C-H and DOH (also referred to as 2,5-DMA), 2C-B and DOB, 2C-C and DOC, 2C-D and DOM, 2C-E and DOET, 2C-I and DOI). Previous findings in literature, obtained with the PLC pathway, also mention increased efficacies for DOx, but show some discrepancies concerning the influence of this substitution on the potency, going from very low potency for both DOx and 2C-X (but even lower for 2C-X) to equipotency between the groups (Blaazer et al. 2008; Moya et al. 2007; Parrish et al. 2005). Within the DOx group, analogously with the 2C-X group, we assessed the effect of the 4-substitution of the most simple compound DOH (2,5-DMA), and of rigidifying the

methoxy groups on the phenyl moiety. The structures of the compounds and the obtained potency and efficacy values are given in Figure 1 and Table 2, and their concentration-response curves in Supplementary Figure S2.

As seen in the 2C-X group, also in the DOx group the unsubstituted compound DOH (2,5-DMA) had the lowest potency and efficacy (EC_{50} of 2814 nM and E_{max} of 107 %). The substitution of DOH (2,5-DMA) with a lipophilic group at position 4 of the phenyl moiety resulted in increased potencies, and small or no increases in the maximal efficacies of the compounds. In this study, this was consistently observed upon substitution with halogens Br, I and Cl, and methyl (DOM) and ethyl (DOET) groups, with potencies in the low nanomolar range and efficacies ranging between 107 and 120 %. Also here, the positive influence of this substitution on the activity of the compounds is in line with literature (Blaazer et al. 2008; Poulie et al. 2019). Furthermore, similarly as in the 2C-X group, replacement of the methyl group in DOM (43.2 nM, 122 %) by an ethyl group in DOET resulted in an increased potency (7.84 nM, 118 %)(Blaazer et al. 2008).

Structurally rigidifying DOB, by incorporation of the two methoxy groups of the phenyl moiety into a fully aromatic benzodifuran core, yields Bromo-DragonFLY, of which the structure is shown in Figure 1 (Parker et al. 1998). Bromo-DragonFLY has been reported to be an exceptionally potent psychedelic, and more potent than DOB in behavioral assays (Halberstadt et al. 2019; Nichols 2018). However, while our values for potency and efficacy (2.95 nM; 120 %) of this substance are the highest reported values within the subgroup of phenylisopropylamines (DOx), these are not significantly different from its structural analogue DOB (3.91 nM; 116 %). Our data thus suggest that the reported higher potency in behavioral assays is not linked to an *intrinsically* higher 5-HT_{2A}R activation potential (at least, not reflected by the βarr2 assay applied here). Other contributing factors *in vivo* may be e.g. the resistance of the structurally rigid analogue to metabolism, as compared to the non-aromatic analogues, and inhibition of monoamine-oxidase A, an enzyme involved in degradation of phenethylamines (Halberstadt et al. 2019; Noble et al. 2018).

3. N-benzylderivatives (25X-NB)

Contrarily to the effect of the introduction of a methyl group at the amine function of a 2C-X compound (thus yielding N-Me-2C-H, discussed in section 1), the introduction of larger benzyl substituents at this position (the NB-derivatives) had a positive influence on the activity of the compounds. The resulting concentration-response curves are shown in Supplementary Figure S3. The possibility of 'solving' the low potency of 2C-H by N-benzyl derivatization has been reported in literature, an observation confirmed by our findings (Blaazer et al. 2008; Braden et al. 2006). More specifically, a strong rise in potency and efficacy can be seen when comparing the EC_{50} and E_{max} of 2C-H (Table 2, 2408 nM and

67.4 %, respectively) with its derivatives 25H-NBF (393 nM; 104 %), 25H-NBMD (with 2',3'-methylenedioxy moiety, 154 nM; 117 %), 25H-NBOH (12.8 nM; 131 %) and 25H-NBOMe (12.8 nM; 144 %). Our ranking order of the potency and efficacy of R^7-substituted compounds, as shown in Figure 1 and Table 2, (NBF < NBMD < NBOH ≈ NBOMe) is consistent with that observed by Jensen *et al.*, who tested a series of 25I-analogues in IP and Ca^{2+} assays, and with the finding of Hansen *et al.* that the –NBF derivatives were overall the least active *N*-benzyl-derived compounds in an IP assay (Hansen et al. 2014; Jensen et al. 2017).

Whereas the substitution at position 4 of the phenyl moiety (R^1) appeared very important in the 2C-X and DOx groups, literature data indicated that this was not as necessary for the activities of the N-benzyl derivatives (Leth-Petersen et al. 2016; Poulie et al. 2019). This finding was confirmed by the data obtained in this study: a strong influence of the R^1 substituent was observed when comparing 2C-H to e.g. 2C-B, but not in the comparison between 25H-NBOMe and 25B-NBOMe. Yet, also within the NBOMe subgroup, with overall low nanomolar potencies and high efficacies, the unsubstituted 25H-NBOMe had the lowest potency for βarr2 recruitment (12.8 nM). A methyl to ethyl switch of the para-alkylsubstituent in the NBOMe group (25D-NBOMe and 25E-NBOMe) did not significantly influence the potency and efficacy in terms of βarr2 recruitment. This contrasts with the findings reported by Rickli *et al.*, who used a FLIPR membrane potential assay and observed for NBOMes an opposite trend to that seen in the 2C-X derivatives (Rickli et al. 2015). The apparent discrepancy between these results can be due to several reasons, as discussed further.

Within all R^1-substituted compounds, the NB derivatives are more potent and efficacious than their counterparts without those extended groups (2C-X), with the NBOMe compounds having the highest efficacy, albeit not significantly higher than the NBOH compounds. The higher potency for NBOMes, as compared to the 2C-X counterparts, is consistent with our previously published findings (Pottie et al. 2019). However, the literature on this topic does not allow for an unambiguous conclusion. In line with our findings are reports by Hansen *et al.*, who found increased binding affinities and low-to-sub nanomolar potencies for NBOMe and NBOH compounds via monitoring PLC-stimulated IP production, and by Braden *et al*., who used an IP turnover assay (Braden et al. 2006; Hansen et al. 2014). In contrast, Rickli *et al.* and Elmore *et al.* reported similar or lower potencies and efficacies when comparing NBOMes and 2C-X compounds using *in vitro* assays monitoring the changes in Ca^{2+} levels (Elmore et al. 2018; Rickli et al. 2015).

4. Correlation of the obtained results with literature and with (estimated) user doses

In general, the observed trends in Table 2 and described above for βarr2 recruitment using the newly developed bioassay, align with previous reports on the structure-activity relationship of psychedelic

compounds at the 5-HT_{2A}R, which is responsible for mediating their typical effects. As noted above, however, there are some discrepancies with data obtained from *in vitro* assays monitoring the changes in Ca^{2+} levels upon activation of the receptor (Elmore et al. 2018; Rickli et al. 2015). On the other hand, the trends observed with the βarr2 recruitment assay do align with those from PLC-mediated changes in IP, and with the affinities obtained from binding assays (Braden et al. 2006; Eshleman et al. 2018; Hansen et al. 2014; Parrish et al. 2005). Possible explanations for discrepancies in results could lie in the use of different cell lines and distinct assay platforms, with associated divergent levels of signal amplification and differential impact of 'receptor reserve', as outlined above. Noteworthy in this context is that both βarr2 recruitment and PLC activation, each independently, are signaling events more upstream than Ca^{2+} release. As a consequence, a 'range' of efficacies can be obtained (with a potential plateauing effect in some assays). Alternatively (or in addition), biased agonism or biased signaling may have an impact on the monitored outcome (Canal 2018; Kurrasch-Orbaugh et al. 2003). A direct comparison of the outcome of βarr2 recruitment assays with that of G protein recruitment assays, applying maximally comparable assay formats, as has been done for other receptors, may help to shed light on this latter aspect (Pottie et al. 2020; Vasudevan et al. 2020; Wouters et al. 2020).

Recently, Luethi and Liechti described the correlation of commonly used doses of psychedelics with binding data, but not with the data obtained with a functional Ca^{2+} assay at the 5-HT_{2A}R. These authors also pointed out the value of *in vitro* pharmacological profiles for the prediction of psychoactive doses and effects of NPS in humans, and the usefulness for the appropriate scheduling of scarcely described compounds (Luethi and Liechti 2018; Luethi and Liechti 2020; Rickli et al. 2015). Here, we used a similar approach, comparing common recreational doses of serotonergic psychedelics, as calculated from PiHKAL and the websites described in Material and Methods, with their potency of inducing βarr2 recruitment to the 5-HT_{2A}R in our newly developed stable cell system (Shulgin and Shulgin 1991). Employing a Pearson correlation analysis, a correlation factor of 0.897 ($P < 0.0001$) was obtained between the EC_{50} (nM) and the estimated dose (mg), as visually depicted in Figure 3. The Figure depicts the clustering of the different subgroups, with 2C-X shown as red dots, DOx shown as green squares (with similar EC_{50} values, though lower doses) and NB-derivatives shown as orange triangles (with lower EC_{50} values and even lower doses). Several substances are not located within these more dense 'clusters': LSD (depicted as a black rhombus), DOH (2,5-DMA) (the grey square, reportedly not inducing psychedelic effects), two compounds indicated in red at the upper right of the graph (mescaline and β-k-2C-B, with higher doses and lower potencies), and Bromo-dragonFLY (green square that has a lower dose than the other DOx substances). This artificial approach certainly has its limitations, because of the impossibility to include variables such as metabolism and bioavailability, and the inherent limitation in assessing the estimated dose. However, the relatively high number of

compounds involved (25 substances, for which potency values were obtained using the same assay) and the high correlation coefficient clearly indicates the usefulness of this functional assay for the characterization of psychedelic phenalkylamines and their effects. Furthermore, (unpublished) data on tryptamines obtained on transiently transfected cells (as depicted by blue inverted triangles), indicate that the observed correlation still holds true when other structural classes are included in the analysis (Pottie et al. 2019; Pottie et al, manuscript in preparation).

Conclusion

In conclusion, we report on the successful development of a cell line stably expressing 5-HT_{2A}R-LgBiT and SmBiT-βarr2. This cell line allows the assessment of a receptor-proximal event, in this case βarr2 recruitment to the activated 5-HT_{2A}R, using the principle of functional complementation of a split nanoluciferase. Using a subset of compounds, this cell line was shown to yield similar EC_{50} and E_{max} values as those obtained using a previously reported system based on transient transfection of cells. Moreover, the stable cell system offers the advantage of a reduction in assay time and the variability inherently induced by differences in transfection efficiency. This stable *in vitro* bioassay system was used for the simultaneous functional characterization of a set of 30 phenylalkylamine psychedelics. These encompassed three different subclasses: 12 phenethylamines (2C-X), 7 phenylisopropylamines (psychedelic amphetamines, DOx) and 11 N-benzylderivatives (25X-NB), allowing for the comprehensive assessment of the structure-activity relationship within and between different subclasses. In general, the obtained findings corresponded with *in vitro* data from literature, and, interestingly, showed a clear correlation with common drug dose estimates. Thus, the assay provides valuable information for the pharmacological characterization of psychedelic NPS at their main target receptor, the 5-HT_{2A}R. Moreover, the obtained data may also allow prioritization of legal actions related to the most potent -and potentially dangerous- compounds.

Acknowledgements

Alexandra Smina is acknowledged for the help during the practical implementation of the experiments. Prof. Kristof Maudens is acknowledged for kindly providing the analytical standards of 2C-B, 2C-C, 2C-I, 25B-NBOMe, 25C-NBOMe and 25I-NBOMe. The authors want to thank Chiron for the generous gift of the analytical standard of Bromo-DragonFLY. C. Stove acknowledges funding by the Research Foundation-Flanders (FWO) [G069419N] and the Ghent University – Special Research Fund (BOF) [01J15517]. A. Cannaert acknowledges funding as a postdoctoral research fellow from the Research Foundation Flanders (FWO; 12Y9520N) and the Ghent University Special Research Fund (BOF; PDO026-18).

Conflict of interest

The authors declare that they have no conflict of interest.

REFERENCES

Blaazer AR, Smid P, Kruse CG (2008) Structure-activity relationships of phenylalkylamines as agonist ligands for 5-HT(2A) receptors. ChemMedChem 3(9):1299-309 doi:10.1002/cmdc.200800133

Braden MR, Parrish JC, Naylor JC, Nichols DE (2006) Molecular interaction of serotonin 5-HT2A receptor residues Phe339(6.51) and Phe340(6.52) with superpotent N-benzyl phenethylamine agonists. Molecular pharmacology 70(6):1956-64 doi:10.1124/mol.106.028720

Canal CE (2018) Serotonergic Psychedelics: Experimental Approaches for Assessing Mechanisms of Action. Handbook of experimental pharmacology 252:227-260 doi:10.1007/164_2018_107

Cannaert A, Franz F, Auwarter V, Stove CP (2017) Activity-Based Detection of Consumption of Synthetic Cannabinoids in Authentic Urine Samples Using a Stable Cannabinoid Reporter System. Analytical chemistry 89(17):9527-9536 doi:10.1021/acs.analchem.7b02552

Cannaert A, Storme J, Franz F, Auwarter V, Stove CP (2016) Detection and Activity Profiling of Synthetic Cannabinoids and Their Metabolites with a Newly Developed Bioassay. Analytical chemistry 88(23):11476-11485 doi:10.1021/acs.analchem.6b02600

Dean BV, Stellpflug SJ, Burnett AM, Engebretsen KM (2013) 2C or not 2C: phenethylamine designer drug review. Journal of medical toxicology : official journal of the American College of Medical Toxicology 9(2):172-8 doi:10.1007/s13181-013-0295-x

Dixon AS, Schwinn MK, Hall MP, et al. (2016) NanoLuc Complementation Reporter Optimized for Accurate Measurement of Protein Interactions in Cells. ACS chemical biology 11(2):400-8 doi:10.1021/acschembio.5b00753

Elmore JS, Decker AM, Sulima A, et al. (2018) Comparative neuropharmacology of N-(2-methoxybenzyl)-2,5-dimethoxyphenethylamine (NBOMe) hallucinogens and their 2C counterparts in male rats. Neuropharmacology 142:240-250 doi:10.1016/j.neuropharm.2018.02.033

EMCDDA-Europol (2014) EMCDDA–Europol Joint Report on a new psychoactive substance 4-iodo-2,5-dimethoxy-N-(2-methoxybenzyl)phenethylamine (25I-NBOMe).

EMCDDA (2004) Report on the risk assessment of 2C-I, 2C-T-2 and 2C-T-7 in the framework of the joint action on new synthetic drugs.

Eshleman AJ, Wolfrum KM, Reed JF, Kim SO, Johnson RA, Janowsky A (2018) Neurochemical pharmacology of psychoactive substituted N-benzylphenethylamines: High potency agonists at 5-HT2A receptors. Biochemical pharmacology 158:27-34 doi:10.1016/j.bcp.2018.09.024

Halberstadt AL, Chatha M, Stratford A, Grill M, Brandt SD (2019) Comparison of the behavioral responses induced by phenylalkylamine hallucinogens and their tetrahydrobenzodifuran ("FLY") and benzodifuran ("DragonFLY") analogs. Neuropharmacology 144:368-376 doi:10.1016/j.neuropharm.2018.10.037

Hansen M, Phonekeo K, Paine JS, et al. (2014) Synthesis and structure-activity relationships of N-benzyl phenethylamines as 5-HT2A/2C agonists. ACS chemical neuroscience 5(3):243-9 doi:10.1021/cn400216u

Hondebrink L, Zwartsen A, Westerink RHS (2018) Effect fingerprinting of new psychoactive substances (NPS): What can we learn from in vitro data? Pharmacology & therapeutics 182:193-224 doi:10.1016/j.pharmthera.2017.10.022

Iwersen-Bergmann S, Lehmann S, Heinemann A, et al. (2019) Mass poisoning with NPS: 2C-E and Bromo-DragonFly. International journal of legal medicine 133(1):123-129 doi:10.1007/s00414-018-1882-9

Jensen AA, McCorvy JD, Leth-Petersen S, et al. (2017) Detailed Characterization of the In Vitro Pharmacological and Pharmacokinetic Properties of N-(2-Hydroxybenzyl)-2,5-Dimethoxy-4-Cyanophenylethylamine (25CN-NBOH), a Highly Selective and Brain-Penetrant 5-HT2A Receptor Agonist. The Journal of pharmacology and experimental therapeutics 361(3):441-453 doi:10.1124/jpet.117.239905

Kolaczynska KE, Luethi D, Trachsel D, Hoener MC, Liechti ME (2019) Receptor Interaction Profiles of 4-Alkoxy-Substituted 2,5-Dimethoxyphenethylamines and Related Amphetamines. Frontiers in pharmacology 10:1423 doi:10.3389/fphar.2019.01423

Kurrasch-Orbaugh DM, Watts VJ, Barker EL, Nichols DE (2003) Serotonin 5-hydroxytryptamine 2A receptor-coupled phospholipase C and phospholipase A2 signaling pathways have different receptor reserves. The Journal of pharmacology and experimental therapeutics 304(1):229-37 doi:10.1124/jpet.102.042184

Kyriakou C, Marinelli E, Frati P, et al. (2015) NBOMe: new potent hallucinogens - pharmacology, analytical methods, toxicities, fatalities: a review. Eur Rev Med Pharmaco 19(17):3270-3281

Leth-Petersen S, Petersen IN, Jensen AA, et al. (2016) 5-HT2A/5-HT2C Receptor Pharmacology and Intrinsic Clearance of N-Benzylphenethylamines Modified at the Primary Site of Metabolism. ACS chemical neuroscience 7(11):1614-1619 doi:10.1021/acschemneuro.6b00265

Lopez-Gimenez JF, Gonzalez-Maeso J (2018) Hallucinogens and Serotonin 5-HT2A Receptor-Mediated Signaling Pathways. Current topics in behavioral neurosciences 36:45-73 doi:10.1007/7854_2017_478

Luethi D, Liechti ME (2018) Monoamine Transporter and Receptor Interaction Profiles in Vitro Predict Reported Human Doses of Novel Psychoactive Stimulants and Psychedelics. The international journal of neuropsychopharmacology 21(10):926-931 doi:10.1093/ijnp/pyy047

Luethi D, Liechti ME (2020) Designer drugs: mechanism of action and adverse effects. Archives of toxicology doi:10.1007/s00204-020-02693-7

Luethi D, Trachsel D, Hoener MC, Liechti ME (2018) Monoamine receptor interaction profiles of 4-thio-substituted phenethylamines (2C-T drugs). Neuropharmacology 134(Pt A):141-148 doi:10.1016/j.neuropharm.2017.07.012

Luethi D, Widmer R, Trachsel D, Hoener MC, Liechti ME (2019) Monoamine receptor interaction profiles of 4-aryl-substituted 2,5-dimethoxyphenethylamines (2C-BI derivatives). European journal of pharmacology 855:103-111 doi:10.1016/j.ejphar.2019.05.014

Moya PR, Berg KA, Gutierrez-Hernandez MA, et al. (2007) Functional selectivity of hallucinogenic phenethylamine and phenylisopropylamine derivatives at human 5-hydroxytryptamine (5-HT)2A and 5-HT2C receptors. The Journal of pharmacology and experimental therapeutics 321(3):1054-61 doi:10.1124/jpet.106.117507

Nichols DE (2004) Hallucinogens. Pharmacology & therapeutics 101(2):131-81 doi:10.1016/j.pharmthera.2003.11.002

Nichols DE (2016) Psychedelics. Pharmacological reviews 68(2):264-355 doi:10.1124/pr.115.011478

Nichols DE (2018) Chemistry and Structure-Activity Relationships of Psychedelics. Current topics in behavioral neurosciences 36:1-43 doi:10.1007/7854_2017_475

Noble C, Holm NB, Mardal M, Linnet K (2018) Bromo-dragonfly, a psychoactive benzodifuran, is resistant to hepatic metabolism and potently inhibits monoamine oxidase A. Toxicol Lett 295:397-407 doi:10.1016/j.toxlet.2018.07.018

Parker MA, Marona-Lewicka D, Lucaites VL, Nelson DL, Nichols DE (1998) A novel (benzodifuranyl)aminoalkane with extremely potent activity at the 5-HT2A receptor. Journal of medicinal chemistry 41(26):5148-9 doi:10.1021/jm9803525

Parrish JC, Braden MR, Gundy E, Nichols DE (2005) Differential phospholipase C activation by phenylalkylamine serotonin 5-HT 2A receptor agonists. Journal of neurochemistry 95(6):1575-84 doi:10.1111/j.1471-4159.2005.03477.x

Pottie E, Cannaert A, Van Uytfanghe K, Stove CP (2019) Setup of a Serotonin 2A Receptor (5-HT2AR) Bioassay: Demonstration of Its Applicability To Functionally Characterize Hallucinogenic New Psychoactive Substances and an Explanation Why 5-HT2AR Bioassays Are Not Suited for Universal Activity-Based Screening of Biofluids for New Psychoactive Substances. Analytical chemistry 91(24):15444-15452 doi:10.1021/acs.analchem.9b03104

Pottie E, Tosh DK, Gao ZG, Jacobson KA, Stove CP (2020) Assessment of biased agonism at the A3 adenosine receptor using beta-arrestin and miniGalphai recruitment assays. Biochemical pharmacology 177:113934 doi:10.1016/j.bcp.2020.113934

Poulie CBM, Jensen AA, Halberstadt AL, Kristensen JL (2019) DARK Classics in Chemical Neuroscience: NBOMes. ACS chemical neuroscience doi:10.1021/acschemneuro.9b00528

Rickli A, Luethi D, Reinisch J, Buchy D, Hoener MC, Liechti ME (2015) Receptor interaction profiles of novel N-2-methoxybenzyl (NBOMe) derivatives of 2,5-dimethoxy-substituted phenethylamines (2C drugs). Neuropharmacology 99:546-53 doi:10.1016/j.neuropharm.2015.08.034

Rickli A, Moning OD, Hoener MC, Liechti ME (2016) Receptor interaction profiles of novel psychoactive tryptamines compared with classic hallucinogens. European neuropsychopharmacology : the journal of the European College of Neuropsychopharmacology 26(8):1327-37 doi:10.1016/j.euroneuro.2016.05.001

Shulgin A, Shulgin A (1991) PiHKAL: A chemical Love Story

Suzuki J, Dekker MA, Valenti ES, et al. (2015) Toxicities associated with NBOMe ingestion-a novel class of potent hallucinogens: a review of the literature. Psychosomatics 56(2):129-39 doi:10.1016/j.psym.2014.11.002

UNODC (2020) Current NPS Threats.

Vasudevan L, Vandeputte M, Deventer M, Wouters E, Cannaert A, Stove CP (2020) Assessment of structure-activity relationships and biased agonism at the Mu opioid receptor of novel synthetic opioids using a novel, stable bio-assay platform. Biochemical pharmacology 177:113910 doi:10.1016/j.bcp.2020.113910

Wacker D, Wang S, McCorvy JD, et al. (2017) Crystal Structure of an LSD-Bound Human Serotonin Receptor. Cell 168(3):377-389 e12 doi:10.1016/j.cell.2016.12.033

Wouters E, Walraed J, Banister SD, Stove CP (2019) Insights into biased signaling at cannabinoid receptors: synthetic cannabinoid receptor agonists. Biochem Pharmacol 169:113623 doi:10.1016/j.bcp.2019.08.025

Wouters E, Walraed J, Robertson MJ, et al. (2020) Assessment of Biased Agonism among Distinct Synthetic Cannabinoid Receptor Agonist Scaffolds. ACS pharmacology & translational science 3(2):285-295 doi:10.1021/acsptsci.9b00069

FIGURES

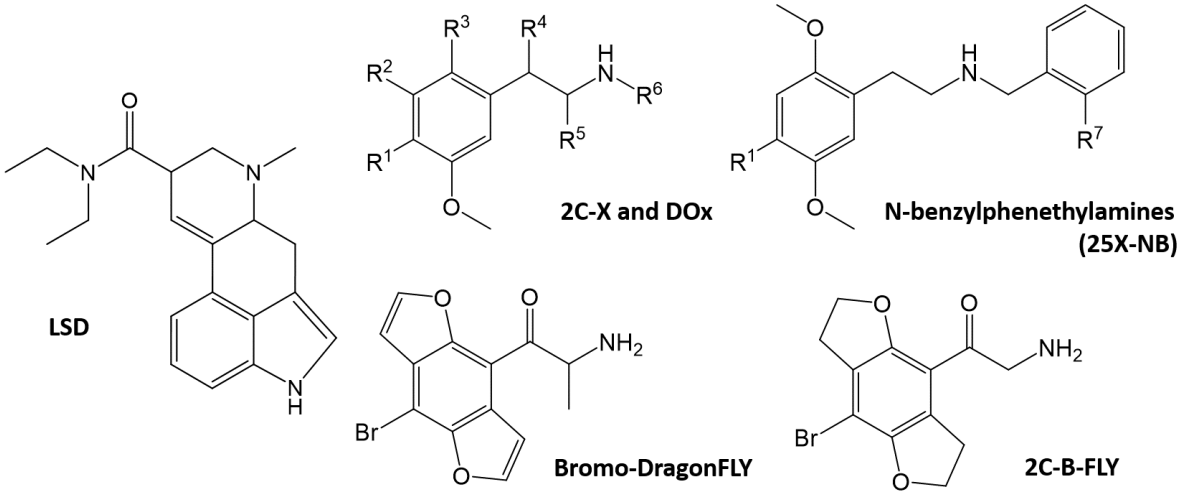

Figure 1: Chemical structures of the tested compounds. The R-groups refer to the substitutions as marked in Table 2.

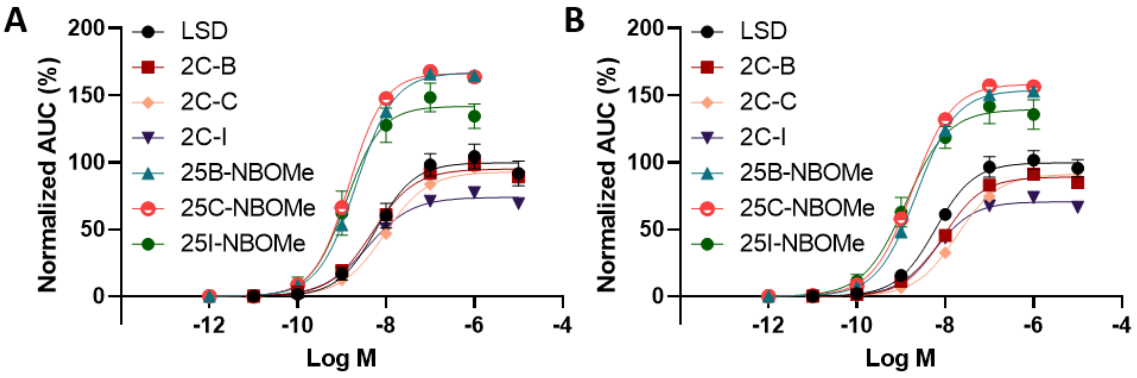

Figure 2: (A) Sigmoidal concentration-response curves of 5-HT_{2A}R agonists serotonin and LSD, obtained with the newly developed stable cell system. (B) Comparison of the activation profiles of the highest concentrations (10^{-5} M) of serotonin and LSD in the developed stable cell system, of one representative experiment. (C and D) Resulting concentration-response curves using either cells transiently transfected with the 5-HT_{2A} receptor and βarr2 constructs (panel C), or the cell line stably expressing the same fusion proteins (panel D). Data are given as the mean of three independent experiments (except for panel B, showing the result of one representative experiment), each performed in duplicate, ± SEM (standard error of the mean). AUC is normalized for the maximal AUC of reference agonist LSD (100 %).

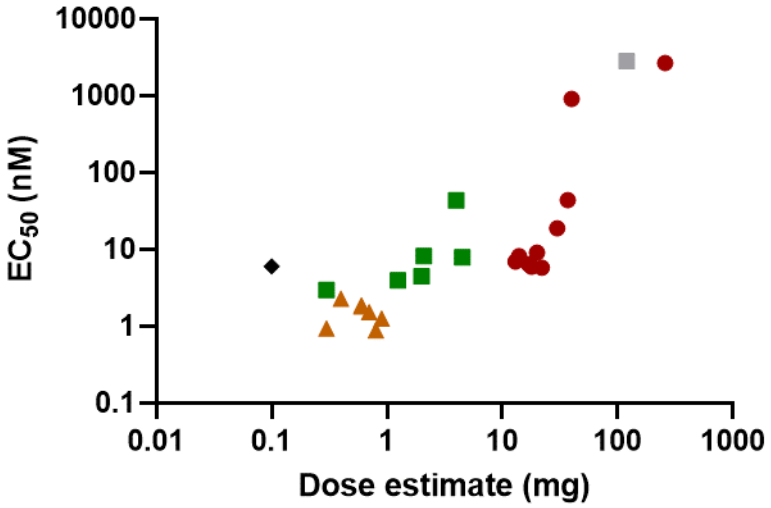

Figure 3: Visual representation of the analysis of the correlation between the EC_{50} values obtained in the stable 5-HT_{2A}R – βarr2 recruitment assay, and the dose estimates for recreational use. A Pearson analysis revealed a correlation factor of 0.897 ($P < 0.0001$). The red dots represent the phenethylamine substances (2C-X and mescaline), the green squares the phenylisopropylamines (DOx and Bromo-DragonFLY), and the orange triangles the N-benzyl-derived compounds (-NBOMe and NBOH). The grey square refers to DOH (2,5-DMA), for which a "common dose" was reported in PIHKAL, despite the lack of psychedelic effects. The blue inverted triangles represent four tryptamines, included in the figure to show the translatability of the correlation to other compound classes.

TABLES

Table 1: Table summarizing the obtained parameters for potency (EC_{50}) and efficacy (E_{max}) for each of the compounds in both the bioassay using transiently transfected cells, and the assay employing the newly developed stable cell system. Data are from three independent experiments, each performed in duplicate. CI: 95% confidence interval.

	Transient transfection		Stable cell system	
Compound	**EC_{50} (nM) (CI)**	**E_{max} (%) (CI)**	**EC_{50} (nM) (CI)**	**E_{max} (%) (CI)**
LSD	5.96 (3.19 – 10.7)	100 (90.8 – 110)	5.95 (3.94 - 8.84)	100 (93.6 - 106)
2C-B	4.86 (3.21 – 7.29)	95.0 (89.3 – 101)	9.03 (6.73 - 12.1)	89.0 (84.7 - 93.4)
2C-C	9.27 (6.09 – 14.3)	92.9 (86.8 – 99.6)	18.7 (15.0 - 23.5)	91.2 (87.7 - 94.7)
2C-I	3.83 (2.10 – 7.01)	73.9 (67.7 – 80.6)	5.91 (4.01 - 8.59)	70.6 (66.5 - 75.0)

25B-NBOMe	2.11 (1.48 – 3.07)	167 (156 – 178)	2.27 (1.62 - 3.23)	154 (145 - 163)
25C-NBOMe	1.46 (1.05 – 2.13)	167 (156 – 178)	1.81 (1.19 - 2.84)	158 (147 - 171)
25I-NBOMe	1.25 (0.75 – 2.22)	142 (129 – 156)	1.29 (0.766 – 2.30)	139 (128 - 153)

Table 2: Summary of the potency (EC_{50}) and efficacy (E_{max}, where the E_{max} of LSD is set to 100 %) values of all the tested compounds. For every compound, the Table shows the substitutions of the basic structures as provided in Figure 1. For the compounds for which no substituents are given (LSD, 2C-B-FLY and Bromo-DragonFLY), the full structures are provided in Figure 1. CI: 95% confidence interval.

Compound	**R^1 (X)**	**R^2**	**R^3**	**R^4 (β)**	**R^5 (α)**	**R^6**	**R^7**	**EC_{50} (nM) (CI)**	**E_{max} (%) (CI)**
LSD								5.95 (3.94 - 8.84)	100 (93.6 - 106)
Mescaline	OCH_3	OCH_3	-	-	-	H		2659 (1732 - 3788)	55.5 (51.3 - 60.3)
				Phenethylamines (2C-X)					
2C-H	H	-	OCH_3	-	-	H		2408 (1844 - 3378)	67.4 (62.3 - 74.7)
2C-B	Br	-	OCH_3	-	-	H		9.03 (6.73 - 12.1)	89.0 (84.7 - 93.4)
β-k-2C-B	Br	-	OCH_3	O=	-	H		905 (548 - 2060)	40.8 (36.3 - 50.1)
2C-B-FLY								8.11 (5.06 - 12.8)	81.8 (75.9 - 88.1)
2C-C	Cl	-	OCH_3	-	-	H		18.7 (15.0 - 23.5)	91.2 (87.7 - 94.7)
2C-D	CH_3	-	OCH_3	-	-	H		43.5 (21.4 - 93.7)	78.7 (69.3 - 91.0)
2C-E	C_2H_5	-	OCH_3	-	-	H		6.88 (3.55 - 12.5)	83.5 (75.5 - 92.3)
2C-I	I	-	OCH_3	-	-	H		5.91 (4.01 - 8.59)	70.6 (66.5 - 75.0)
N-Me-2C-H	H	-	OCH_3	-	-	CH_3		4464 (2094 - 8109)	41.2 (34.5 - 50.9)
2C-T-2	SC_2H_5	-	OCH_3	-	-	H		6.42 (4.03 - 10.3)	106 (98.5 - 114)
2C-T-7	SC_3H_7	-	OCH_3	-	-	H		5.76 (2.10 - 30.4)	101 (84.7 - 134)
				Phenylisopropylamines (DOx)					
DOB	Br	-	OCH_3	-	CH_3	H		3.91 (2.41 - 6.35)	116 (109 - 125)

DOC	Cl	-	OCH_3	-	CH_3	H	8.14 (5.3 - 12.7)	107 (100 - 115)
DOM	CH_3	-	OCH_3	-	CH_3	H	43.2 (27.4 - 72.5)	122 (113 - 134)
DOET	C_2H_5	-	OCH_3	-	CH_3	H	7.84 (5.66 - 10.9)	118 (112 - 124)
DOI	I	-	OCH_3	-	CH_3	H	4.43 (1.48 - 27.9)	112 (92.9 - 152)
DOH	H	-	OCH_3	-	CH_3	H	2814 (1801 - 4777)	107 (95.8 - 122)
Bromo-dragonFLY							2.95 (1.57 - 5.81)	120 (108 - 135)
				N-benzylphenethylamines (25X-NB)				
25B-NBOMe	Br					OCH_3	2.27 (1.62 - 3.23)	154 (145 - 163)
25C-NBOH	Cl					OH	0.897 (0.54 - 1.54)	142 (131 - 154)
25C-NBOMe	Cl					OCH_3	1.81 (1.19 - 2.84)	158 (147 - 171)
25D-NBOMe	CH_3					OCH_3	1.25 (0.74 - 2.22)	148 (136 - 163)
25E-NBOMe	C_2H_5					OCH_3	0.929 (0.398 - 2.48)	157 (137 - 184)
25I-NBOH	I					OH	1.52 (0.641 - 4.19)	136 (116 - 162)
25I-NBOMe	I					OCH_3	1.29 (0.766 – 2.30)	139 (128 - 153)
25H-NBOH	H					OH	12.8 (7.82 - 21.5)	131 (120 - 142)
25H-NBF	H					F	393 (220 - 735)	104 (92.2 - 119)
25H-NBOMe	H					OCH_3	12.8 (7.52 - 21.7)	144 (133 - 156)
25H-NBMD	H						154 (114 - 221)	117 (108 - 127)

Correction to: *In vitro* structure-activity relationship determination of 30 psychedelic new psychoactive substances by means of β-arrestin 2 recruitment to the serotonin 2A receptor

It has been brought to the authors' attention that Fig. 1 of "In vitro structure-activity relationship determination of 30 psychedelic new psychoactive substances by means of β-arrestin 2 recruitment to the serotonin 2A receptor" contained a mistake in the structures for 2C-B-FLY and Bromo-DragonFLY. This has now been corrected. The authors apologize for any inconvenience caused.

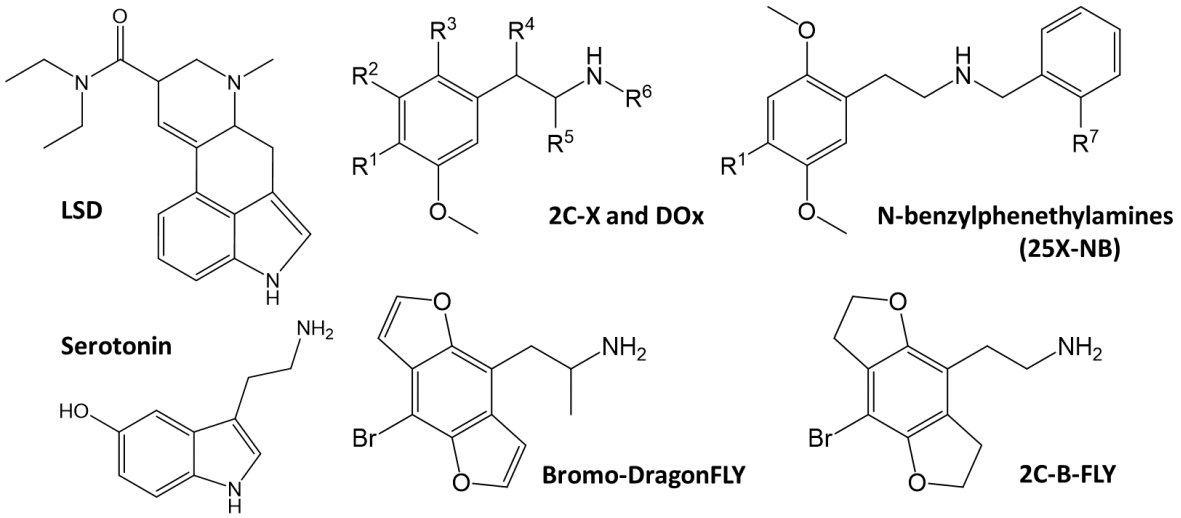

Fig. 1 Chemical structures of the tested compounds. The R-groups refer to the substitutions as marked in Table 2.